Arabian Sea - A Memory Bank for The Indian Summer Monsoon Signals

Vikas Kumar Kushwaha[1], Ashok Karumuri[2], and Feba Francis[1]

[1]University of Hyderabad
[2]CEOAS, University of Hyderabad

November 21, 2022

Abstract

Indian Summer and Winter monsoon winds are major drivers of the mixed layer processes in the Arabian Sea. Our study shows that the Arabian Sea 'traps' the Indian Summer Monsoon (ISM) signal in the sub-surface till the spring of the following year. We find maximum correlations of Indian Summer Monsoon with Arabian sea temperature in the following April. This memory is a consequence of the asymmetry between the summer and winter monsoons. During ISM, the strong westerlies cause a negative wind stress curl over central Arabian Sea sinking the signal to ˜130m deep. In the winter monsoon, the winds are weaker and the signal remains in the subsurface as the mixed layer is still deep. The following spring, the mixed layer becomes shallower and hence the signal resurfaces. The resurfacing signal makes the Arabian Sea a memory bank for the Indian summer Monsoon.

Arabian Sea - A Memory Bank for The Indian Summer Monsoon Signals

Vikas Kumar Kushwaha[1*], Karumuri Ashok[1], Feba Francis[1]

[1]University of Hyderabad

*kushwaha.vikas@outlook.com

Key Points:

- The Arabian Sea 'traps' the Indian Summer Monsoon (June- September) signal in its sub-surface till the following February-March.
- Surface temperature in the Arabian sea during April-May is significantly correlated with the previous Indian summer monsoon rainfall.
- Impact of disparate seasonal processes on the mixed layer, from boreal summer through spring of the following year, cause this.

ABSTRACT

Indian Summer and Winter monsoon winds are major drivers of the mixed layer processes in the Arabian Sea. Our study shows that the Arabian Sea 'traps' the Indian Summer Monsoon (ISM) signal in the sub-surface till the spring of the following year. We find maximum correlations of Indian Summer Monsoon with Arabian sea temperature in the following April. This memory is a consequence of the asymmetry between the summer and winter monsoons. During ISM, the strong westerlies cause a negative wind stress curl over central Arabian Sea sinking the signal to ~130m deep. In the winter monsoon, the winds are weaker and the signal remains in the subsurface as the mixed layer is still deep. The following spring, the mixed layer becomes shallower and hence the signal resurfaces. The resurfacing signal makes the Arabian Sea a memory bank for the Indian summer Monsoon.

Plain Language Summary

The Indian Summer and Winter Monsoons are the prominent drivers of the mixed layer processes in the Northern Indian Ocean. Several studies have shown the impacts of the summer Monsoon and the winter Monsoon on the Arabian Sea individually. However, no study has, so far, shown the impacts caused by the asymmetry of the two Monsoons on the Arabian Sea. Our study shows that the asymmetry in the Monsoons help the Arabian Sea to retain a memory of the Indian Summer Monsoon (ISM) for about 9 months till April of the following year.

Our results are useful for the monsoon prediction and to understand the biogeochemistry of the Arabian Sea.

1. INTRODUCTION

The Indian Summer Monsoon [ISM, June – September (JJAS)] is the most prominent monsoon system. It primarily affects the Indian subcontinent and its surrounding water bodies of the Arabian Sea (AS) and Bay of Bengal (BoB). It accounts for 80% of annual precipitation over India, and 60% of agriculture sector jobs [Webster et al., 1998; Gadgil and Gadgil, 2006]. Besides being an atmospheric phenomenon of considerable societal importance, the ISM winds are the primary driver of near-surface circulation and surface mixed-layer processes of the North Indian Ocean, approximately north of 10°S. The ISM surface winds originate in the region of the Mascarene High as southeasterlies, cross the equator and over the north Indian basin and surrounding their overall direction of flow is south-westerly [Rao, 1964; Rao and Desai, 1971; Saha, 1970; Pathak et al., 2017; Singh et al., 2019]. Further north, in the western AS, the ISM, also known as the southwest monsoon owing to the wind direction in this region, manifests as a strong but narrow core of south-westerlies known as the Findlater jet [Findlater, 1969].

In May, prior to the onset of ISM, the Sea Surface Temperature (SST) in the AS is more or less above the threshold for convection. During mid-May, the SST near Somalia coast increases along the northeastward direction. From an average of 29 ^{0}C near Somalis, the SST reaches to the about 31 ^{0}C near the coast of India. The surface winds near the Somalia coast in the pre-monsoon period are weak, and there is no upwelling along the coast of Somalia. The conditions start changing towards the end of May, with the onset of the ISM.

During the northeast monsoon (NEM), the surface winds over the AS are weaker as compared to the ISM, and spread over a relatively broader region. The NEM induces westward surface currents in the Central Arabian Sea (CAS) [McCreary and Shetye, 1996; Schott et al., 1997]. Consequently, the

SST of the northwestern Arabian Sea (NWAS) and CAS cool in the months of October-December. The mixed layer is more in-depth in these regions during monsoon seasons [Weller et al., 2002] compared to the non-monsoonal seasons, and it is deepest during the northeast monsoon. This manifests as a semi-annual cycle in the thermohaline structure of the upper ocean in the CAS and NWAS, which is unique to these regions. After the NEM season (i.e., the Spring Season - February, March, and April), the surface winds are very weak. These weak winds, with clear skies, leading to the heating of the ocean surface. Because of this, the mixed layer gets shallower and sometimes altogether disappears in CAS [Weller et al., 2002]. Various studies suggest that other processes contribute to the semi-annual cycle of the vertical structure of the upper ocean in these regions [Duing and Leetmaa, 1980; Rao, 1986; McCreary et al., 1993], but the role of monsoons is a dominant one.

Various studies already focused on understanding the dynamics of coastal circulation in north Indian ocean during different seasons [McCreary and W Han 1999, Shankar and McCreary1996, Shetye 1998, Schott and McCreary, 2001]. Importantly, no studies have explored the potential relevance of the asymmetry in the strength of the southwest and northeast monsoons on the sub-surface temperature structure of the Arabian sea. Indeed, no studies have examined the potential implication of the ISM on the sub-surface conditions in the AS beyond the southwest monsoon. Therefore, the main objective of the current study is to explore the response of the sub-surface Arabian Sea to the ISM and its longevity and the potential background processes.

This paper is organized as follows. In the next section, we describe the data used in the study. Section 3 presents the main results of our analysis. Section 4 discusses the conclusions of the study.

2. DATA AND METHODS

We have used Hadley Centre Global Sea Ice and Sea Surface Temperature [HadISST, Rayner et al., 2003] dataset for SST, and the Simple Ocean Data Assimilation ocean/sea ice reanalysis Version 3.3.1 [SODA 3.3.1, Carton et al., 2018] to carry out subsurface analysis. We have also analysed the wind stress data from SODA 3.3.1. For precipitation, we used the gridded data derived from the rain gauge measurements from Indian Meteorological Department (IMD) [Rajeevan et al., 2009].

For reconfirmation of our results, we have also repeated our analysis of the above datasets with Extended Reconstructed Sea Surface Temperature (ERSST) [Huang et al., 2017], Ocean Reanalysis System [ORAS4, Balmaseda et al., 2013] by European Centre for Medium-range Weather Forecasts (ECMWF), Global Ocean Data Assimilation System [GODAS, Behringer et al., 2004], Global Ocean ARGO dataset [Shaolei Lu et al., 2020], and Global Precipitation Climatology Project (GPCP) [Adler et al., 2003], as applicable.

Our study period is from 1980 to 2015, owing to the availability of SODA 3.3.1 data. We have detrended the data for the given period to remove any linear trends. Furthermore, we use the well-known linear anomaly correlation analysis. The statistical significance of the correlations is obtained through a 2-tailed Student’s t-test. We also define an area-averaged Indian summer monsoon rainfall index, referred to as the ISMR. This is obtained by the area-averaging of accumulated JJAS summer rainfall over only the land regions in the domain bound by 66.5 ^{0}E, 100 ^{0}E , 6.5 ^{0}N, 30 ^{0}N [Correlation coeffiecient of IMD gridded rainfall and GPCP bounded by this region is 0.69).

Lastly, the Ekman pumping is calculated as follows:

$$\frac{\partial}{\partial x}(u_E) + \frac{\partial}{\partial y}(v_E) = w_E$$

$$w_E = \nabla \times \frac{\tau}{\rho f}$$

where,

u_E, v_E and w_E are the zonal, meridional and vertical components of Ekman transport,

τ is the wind stress (N/m^3/s)

ρ is the density (1035 kg/m^3),

f is the Coriolis parameter, computed as

$f = 2\omega sin\phi$, where ϕ varies from 15^0 N, 20^0 N in our analysis)

3. RESULTS

Over the central north Arabian Sea, the correlations between the ISMR with the concurrent seasonally-averaged SST are weak, and statistically insignificant even at 90% confidence level, when considering the entire season. This is reasonable because while the southwest monsoon is vigorous more or less throughout the season, the intraseasonal variations are very high .

Figure 1 (upper half) shows the lead anomaly correlation of ISMR during June - September (JJAS) with the Sea Surface Temperature (SST) in the Arabian sea from October to January (ONDJ). During October and November months, the SST anomaly (SSTA) of North-Western Arabian Sea

(NWAS) are significantly correlated to the ISMR at 95% confidence level over several regions in the Arabian Sea. But during December and January, most regions in NWAS are negatively correlated to the ISMR at 95% statistical significance.

The lead correlations of ISMR with monthly SST during subsequent year February to May (FMAM) in the AS are shown in Figure 1 (lower half). Figure 1 (lower half) shows that the SST in the NWAS and CAS during these months are negatively correlated with the preceding ISMR at 95% confidence level. Even in the month of April, the SST is negatively, and strongly, correlated with the preceding ISMR. This result has also been re-ascertained using the ERSST and GODAS datasets (Figures not shown). The importance of this lies in the implication that the signal associated with the ISMR is being observed 7-9 months after the ISM. Indeed, such association of the ISMR on the SST is not expected to last for more than one subsequent season, as the air-sea interaction would have smeared the signal much earlier.

Furthermore, the vertical distribution of the correlation values of the ISMR with the concurrent subsurface temperatures of the AS, area-averaged over the region 54°E~63°E, 14°N~18°N is shown in the Figure 2. We also present in the Figure the lag correlations of the ISMR with sub-surface temperatures of the AS during the ONDJ and FMAM seasons. The concurrent correlations of the ISMR with the concurrent sub-surface temperatures are negative, but not even significant at 95% confidence level. Interestingly, the subsurface temperatures of NWAS during the ONDJ months, up to the depth of about 130 meters, are not only negatively correlated with monsoon in the previous season, but also statistically significant at 95% confidence level; the correlations are maximum at a depth of about 50 m. The significant negative correlations are also seen in the months of FMAM, but are confined to only a depth of 10 meters, with maximum correlations seen at the ocean surface (Fig. 2). We also compare the SODA (subsurface temperature) data with the corresponding Argo data, available for the 2004-2009 period which conforms to Figure 2.

The above discussion indicates that the monsoon signal is potentially ‘memorised’ in the sub-surface AS. In the next paragraphs, we present a potential mechanism, which facilitates the observed ‘memory’.

In the northwestern AS, the ISM manifests as a strong but narrow core of southwesterlies known as the Findlater jet [Findlater, 1969]. These strong low level winds blow parallel to the Somali coast along the Arabian Peninsula and result in coastal upwelling. The winds, then, curve off the Oman coast and almost become westerlies. These strong westerlies establish a strong eastward current in the CAS. In addition, these winds result in coastal upwelling off the Arabian Peninsula in the northern AS and open ocean upwelling in CAS due to Ekman pumping which is driven by strong positive wind stress curl to northwest of the Findlater jet with convergence and downwelling to the southeast of the jet.[e.g. Shetye et al., 1994].

In other words, the core of Findlater jet in CAS, which blows eastward, has opposite effects on both sides of the core in the Northern Arabian Sea due to the consequent Ekman transport dynamics. Specifically, this results in upwelling to the left of core and downwelling to the right of core, i.e. to the north and south of Jet core, respectively, as shown in Figure 3. The ensuing change in the vertical velocity in the ocean mixed layer across the core of the Findlater jet leads to the development of a pressure gradient force across ocean surface, as can be inferred from the aforementioned Ekman dynamics (Fig 3). This facilitates a southward movement of the cooler water from left side of core across the jet to its right side. Importantly, the cooler water downwells into deeper layers to the right of the jet core till about 130m.

Fig 4 shows the annual cycle of mixed layer depth in Arabian Sea over the region (54^0E:63^0E; 14^0N:18^0N). The region was chosen because the correlation coefficient value of ISM with SST in AS is maximum in this region as shown in Figure 1. During the ISM months (JJAS), the mixed layer deepens to a depth of about 80 m, which leads to the cooling of SST. This is because, the strong wind stress drives inertially modulated shear at the base of the mixed layer, leading to entrainment and cooling at the surface.

During the inter-monsoon period between the ISM and winter monsoon, the mixed layer becomes shallow to just about 25 m deep. Seen particularly in the month of October, this is due to the warming of the surface layer by local heat fluxes [Weller et al., 2002]. In winter monsoon, the deepening of mixed layer occurs again; the maximum depth of mixed layer in the month of January, for example, is about 80 m. After the winter monsoon, the shallowing of mixed layer occurs again, and it reaches up to the minimum depth of ~10 m in the month of April.

There are two processes that can deepen the mixed layer in the central Arabian Sea during the summer monsoon. The first of these, and strongly supported by a year-long observation campaign in 1994-1995 (Weller et al, 2002) is that the entrainment induced by wind stress deepens the mixed layer to depths of the order of 80m. The second possibility was raised by Bauer et al (1991). According to it the deepening is influenced by action of wind-stress curl in the central Arabian Sea. This deepening occurs simultaneously with southward movement of waters that upwell in the northern Arabian Sea. The upwelling in the north and downwelling in the south of core of Findlater jet is a consequence of the structure of the winds: a strong jet-like flow with positive vorticity in the north and negative vorticity in the south.

From the results so far, we conclude that, due to a net negative wind stress curl (Fig 5) of the Findlater Jet and the resultant Ekman pumping, colder surface water in the NWAS region downwells till a depth 130m during the summer monsoon. Hence, deepening of mixed layer to about 80m occurs and lead to the cooling of SST by 5^0C in the CAS [Weller et al., 2002]. The deepening of mixed layer and cooling of SST depends on the strength of ISM i.e., stronger ISM leads to deeper mixed layer and much colder SST. After the ISM months, there is shallowing of mixed layer occurs in the month of October due to the warming of surface layer by the local heat fluxes in CAS. Once, the dry and cold north easterlies winds and the positive wind stress associated with it are set up subsequently in the winter monsoon during December to February (DJF) from the mountains of South Asia, the Arabian sea experiences heat loss at the surface layer. Due to this convective cooling, the deepening of mixed layer occurs again and the deepest mixed layer of about 80 m is seen in the months of January and February and hence, results in the cooling of SST by 3 ^{0}C [Weller et al., 2002]. However, the inherent strength of the NEM winds over the AS during this season is substantially weaker, and also spread over the larger area as compared to that of the southwest monsoon. So, the wind driven entrainment has very little effect in this period [Weller et al., 2002]. This is because the mixed layer is still deeper while having positive wind stress curl over the entire Arabian sea.

Thus, the inter-monsoon warming of SST, its subsequent cooling and deepening of the winter mixed-layer are independent of ISM. Also, the surface warming and shallowing of mixed layer occurring in pre-monsoon months (i.e., March) are because of intense solar heating or the local heat fluxes and calm winds. By April, when winds start picking up over AS (because precipitation starts in the far east over Bay of Bengal and farther eastward) there is a bit of deepening of the mixed layer in the AS. This deepening erodes the "cap" that had formed earlier, and exposes the underlying water. This water carries the signature of previous ISMR resulting in the observed high correlation of SST with ISMR in April.

4. CONCLUSION

The Arabian Sea SST gets modulated as a net response of the Ekman dynamics associated with the local southwest and succeeding northeast monsoons, and air-sea fluxes, etc. Analysing various reanalysis/observational datasets for the period of 1980-2015, we document a contiguous chain of inherent seasonal processes in the central and north Arabian Sea, from boreal summer through the following year spring, leading to storing of the signature of the Indian summer monsoon in the sub-surface waters for almost an year. Our study ascertains that the SST in the North-Western Arabian Sea (NWAS) and Central Arabian Sea (CAS) during the spring (March - May) are negatively correlated with the Indian summer monsoon rainfall (ISMR) of the previous year. That is, the SST in these regions are not only expected to be anomalously cool during a good monsoon, but continue to be so, even during the subsequent boreal winter and spring seasons. We propose the following mechanism to explain this relationship: during the ISM, the strong Findlater jet induces an upwelling to the north of its core (~ 15^0N as shown in Fig.6 (a)) and downwelling to its south. The cooler upwelled water moves southward of the jet core in the surface Ekman layer. Here, this cooler water downwells vertically downwards up to a depth of ~130 m due to Ekman pumping associated with a negative wind stress curl and deeper mixed layer. However, the strength of the north easterlies during the northeast monsoon, during DJF months, is substantially weak as compared to that of the south westerlies during summer monsoon in these regions. However, the mixed layer in the boreal fall is very deep, with the air-sea fluxes dictating the SST. Therefore, even after the northeast monsoon sets up from the month of November and induces a positive wind stress curl. The signature of the signal of the previous summer monsoon is apparent from the beginning of the boreal spring, in the months of March-April to be specific, due to deepening of mixed layer, which now affects the surface SST because of entrainment of underlying waters which stores the signal of previous ISM. To sum up, as a result of the asymmetry between the magnitude of inter-monsoonal winds as well as the inter-seasonal changes in the mixed layer depth, the central Arabian Sea ‘remembers and stores’ the previous ISM signature for almost 7-8 months, probably the longest of its kind in the tropics.

The results help in prediction of Arabian sea temperatures which have relevance for tropical cyclone prediction, biological oceanography etc. We plan to conduct several sensitivity experiments with an ocean model for an improved understanding of the mechanism and its possible implications of the Arabian Sea on various timescales.

ACKNOWLEDGEMENT

All the authors would like to thank Prof. Satish Shetye for suggesting the problem and his valuable comments during the consultations on this manuscript.

REFERENCES

Adler, R.F., G.J. Huffman, A. Chang, R. Ferraro, P. Xie, J. Janowiak, B. Rudolf, U. Schneider, S. Curtis, D. Bolvin, A. Gruber, J. Susskind, and P. Arkin, 2003: The Version 2 Global Precipitation Climatology Project (GPCP) Monthly Precipitation Analysis (1979-Present). J. Hydrometeor., 4,1147-1167.

Balmaseda MA, Mogensen K, Weaver AT. 2013. Evaluation of the ECMWF ocean reanalysis systemORAS4.Q. J. R. Meteorol. Soc.139: 1132–1161. DOI:10.1002/qj.2063.

Bauer, Sonia & Hitchcock, Gary & Olson, Donald. (1991). Influence of monsoonally-forced Ekman dynamics upon surface layer depth and plankton biomass distribution in the Arabian Sea. Deep Sea Research Part A. Oceanographic Research Papers. 38. 531–553. 10.1016/0198-0149(91)90062-K.

Behringer, D.W., and Y. Xue, 2004: Evaluation of the global ocean data assimilation system at NCEP: The Pacific Ocean. Eighth Symposium on Integrated Observing and Assimilation Systems for Atmosphere, Oceans, and Land Surface, AMS 84th Annual Meeting, Washington State Convention and Trade Center, Seattle, Washington, 11-15. Derber, J.C., and A. Rosati, 1989: A global oceanic data assimilation system. J. Phys. Oceanogr., 19, 1333-1347.

Duing W. and A. Leetmaa (1980) Arabian Sea cooling: a preliminary heat budget, Journal of Physical Oceanography, 10,307-312.

Findlater, J. 1969. Interhemispheric transport of air in the lower troposphere over the western Indian Ocean. Quart. J. R. Met. Soc. 95,400-403

Gadgil, Sulochana, and Siddhartha Gadgil. "The Indian Monsoon, GDP and Agriculture." Economic and Political Weekly 41, no. 47 (2006): 4887-895.

Huang, B., Peter W. Thorne, et. al, 2017: Extended Reconstructed Sea Surface Temperature version 5 (ERSSTv5), Upgrades, validations, and intercomparisons. J. Climate, doi: 10.1175/JCLI-D-16-0836.1.

Carton, J.A., G.A. Chepurin, and L. Chen, 2018a: SODA3: a new ocean climate reanalysis, J. Clim., **31**, 6967-6983, DOI:10.1175/JCLI-D-18-0149.1.

Knox, R., The Indian Ocean: Interaction with the monsoon, in Monsoons, edited by J. S. Fein and P. L. Stephens, 365--398, John Wiley, New York, 1987.

McCreary, J. P., Han, W., Shankar, D., and Shetye, S. R. (1996), Dynamics of the East India Coastal Current: 2. Numerical solutions, J. Geophys. Res., 101(C6), 13993– 14010, doi:10.1029/96JC00560.

McCreary, J.P., S. Zhang, and S.R. Shetye, 1997: Coastal circulations driven by river outflow in a variable-density 1½-layer model. J. Geophys. Res., **102,** 15,535-15,554.

McCreary, J. P., P. K.Kundu, and R. L.Molinari, 1993: A numerical investigation of dynamics, thermodynamics and mixed-layer processes in the Indian Ocean.Prog. Oceanogr., 31**,** 181–244.

Narayanan, M. S. and Rao, B. M.: Stratification and convection over Arabian Sea during monsoon 1979 from satellite data, P. Indian A. S.-Earth, 98, 339–352, 1989.

Pathak, A., Ghosh, S., Alejandro Martinez, J., Dominguez, F., & Kumar, P. (2017). Role of oceanic and land moisture sources and transport in the seasonal and interannual variability of summer monsoon in India. Journal of Climate, 30, 1839–1859. https://doi.org/10.1175/JCLI-D-16-0156.1

Pai et al. (2014). Pai D.S., Latha Sridhar, Rajeevan M., Sreejith O.P., Satbhai N.S. and Mukhopadhyay B., 2014: Development of a new high spatial resolution (0.25° X 0.25°)Long period (1901-2010) daily gridded rainfall data set over India and its comparison with existing data sets over the region; MAUSAM, 65, 1(January 2014), pp1-18.

Rajeevan M, Bhate J. 2009. A high resolution daily gridded rainfall dataset (1971-2005) for mesoscale meteorological studies. Curr. Sci. 96(4): 558– 562.

Rao R R 1986 Cooling and deepening of the mixed layer in the central Arabian Sea during MONSOON-77: observations and simulations;Deep Sea Res. 33 1413–1424.

Rao, Y. P. 1964. Interhemispheric circulation. Quart. J, R. Met. Soc. 90, 190-194.

Rao, Y. P. and Desai, B. N. 1971. Origin of the southwest monsoon current over the Indian seas. Vayu Mandal 1, No. 1,34-36.

Rayner, N. A.; Parker, D. E.; Horton, E. B.; Folland, C. K.; Alexander, L. V.; Rowell, D. P.; Kent, E. C.; Kaplan, A. (2003) Global analyses of sea surface temperature, sea ice, and night marine air temperature since the late nineteenth century J. Geophys. Res.Vol. 108, No. D14, 4407 10.1029/2002JD002670.

Saha, K. R. 1970. Air and water vapour transport across the equator in the western Indian Ocean during northern summer. Tellus 22,681-687.

Schott, F., J. Fischer, U. Garternicht and D. Quadfasel (1997): Summer monsoon response of the northern Somali current, 1995. Geophys. Res. Let., 24, 2565-2568.

Schott and McCreary, 2001 F. Schott, J.P. McCreary The monsoon circulation of the Indian Ocean Progress in Oceanography, 51 (2001), pp. 1-123.

Shaolei Lu, Zenghong Liu, Hong Li, Zhaoqin Li, Xiaofen Wu, Chaohui Sun, Jianping Xu.(2020). Manual of Global Ocean Argo gridded data set (BOA_Argo) (Version 2020), 15 pp.

Shankar, D., McCreary, J. P., Han, W., and Shetye, S. R. (1996), Dynamics of the East India Coastal Current: 1. Analytic solutions forced by interior Ekman pumping and local alongshore winds, J. Geophys. Res., 101(C6), 13975– 13991, doi:10.1029/96JC00559.

Shetye, S.R., Gouveia, A.D. & Shenoi, S.S.C. Circulation and water masses of the Arabian Sea. Proc. Indian Acad. Sci. (Earth Planet Sci.) **103,** 107–123 (1994). https://doi.org/10.1007/BF02839532.

Shetye and Gouveia, 1998 S.R. Shetye, A.D. Gouveia Coastal circulation in the north Indian Ocean. Coastal segment (14,S-W) The Sea, Vol. 11, John Wiley and Sons, Inc (1998), pp. 523-556

Singh, S., Valsala, V., Prajeesh, A. G., & Balasubramanian, S. (2019). On the variability of Arabian Sea mixing and its energetics. Journal of Geophysical Research: Oceans, 124, 7817– 7836. https://doi.org/10.1029/2019JC015334

Webster, P. J., Magaña, V. O., Palmer, T. N., Shukla, J., Tomas, R. A., Yanai, M., and Yasunari, T. (1998), Monsoons: Processes, predictability, and the prospects for prediction, J. Geophys. Res., 103(C7), 14451– 14510, doi:10.1029/97JC02719.

Weller, R. A., A. S. Fischer, D. L. Rudnick, C. C. Eriksen, T. D. Dickey, J. Marra, C. Fox, and R. Leben (2002), Moored observations of upper-ocean response to the monsoons in the Arabian Sea during 1994–1995, Deep Sea Res., Part II, 49, 2195–2230, doi:10.1016/S0967-0645(02)00035-8.

Fig.1- Correlation of ISMR with SST during the following Oct- May period.

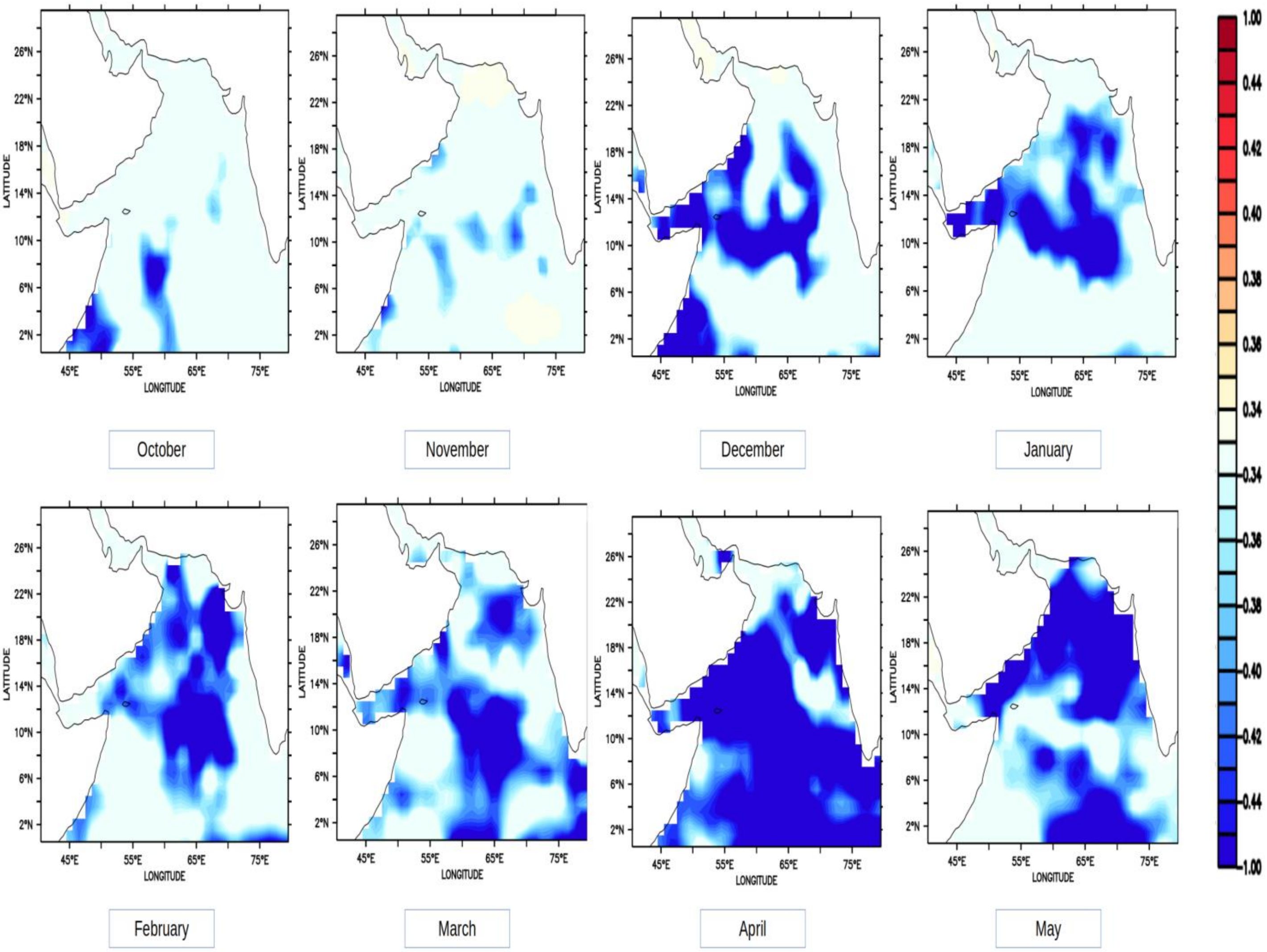

Fig.2- Correlation of ISMR with vertical sub-surface temperature profile (area-averaged over 54 ^{0}E – 63 ^{0}E, 14 ^{0}N- 18 ^{0}N) for the concurrent season (Purple), following October-January (Red), and following February-May (Blue). The yellow line represents the correlations statitsically significant at 95% confidence level (***0.34***).

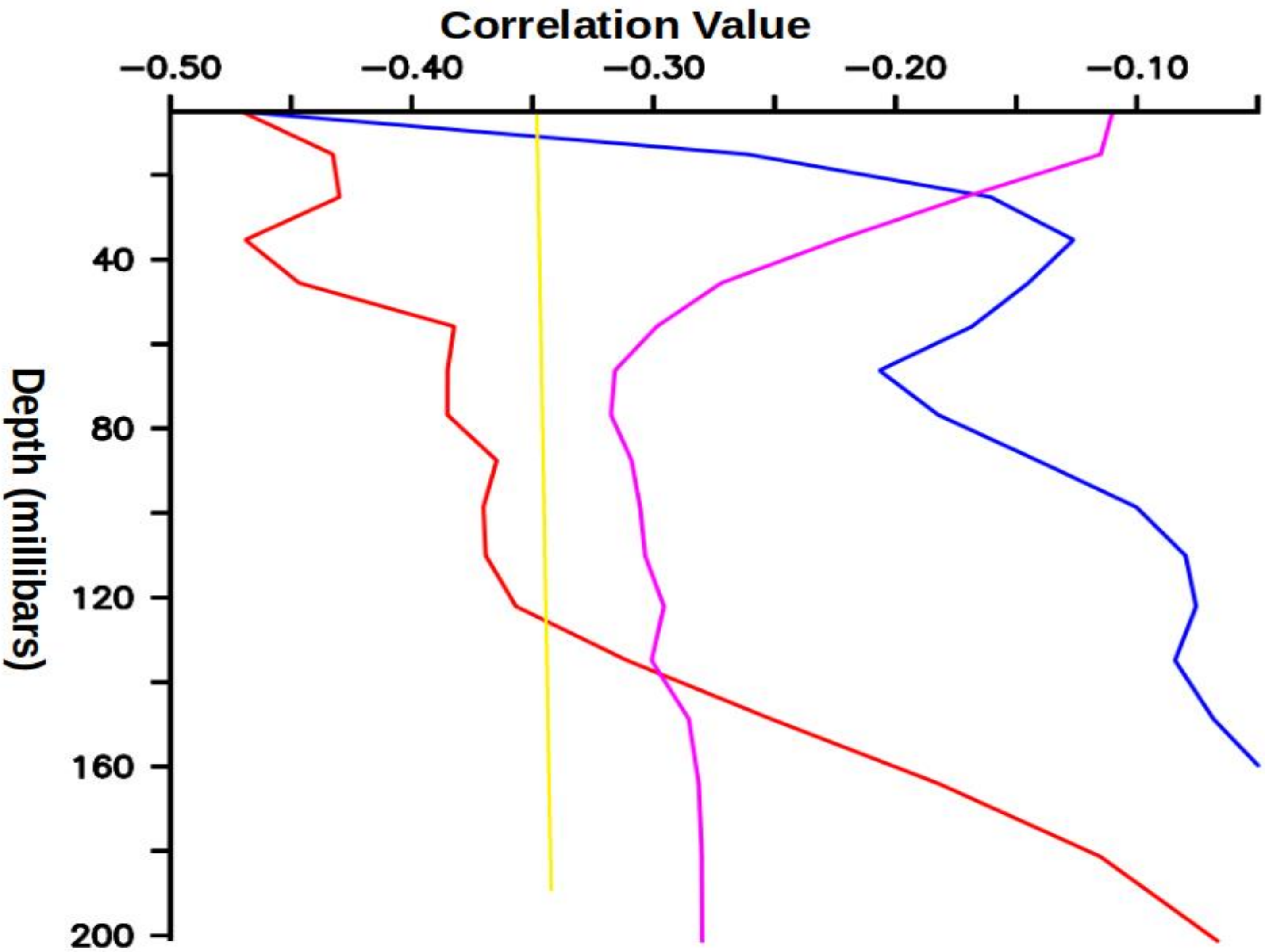

Fig.3- Ekman transport to the south and north of the JJAS Findlater Jet Core in the north Arabian Sea. The values to the north (in red) are obtained by averaging it over 54 ^{0}E- 63 ^{0}E, 16 ^{0}N-20 ^{0}N, and that to the south (in blue) are obtained by averaging it over 54 ^{0}E:83 ^{0}E; 10 ^{0}N:14 ^{0}N.

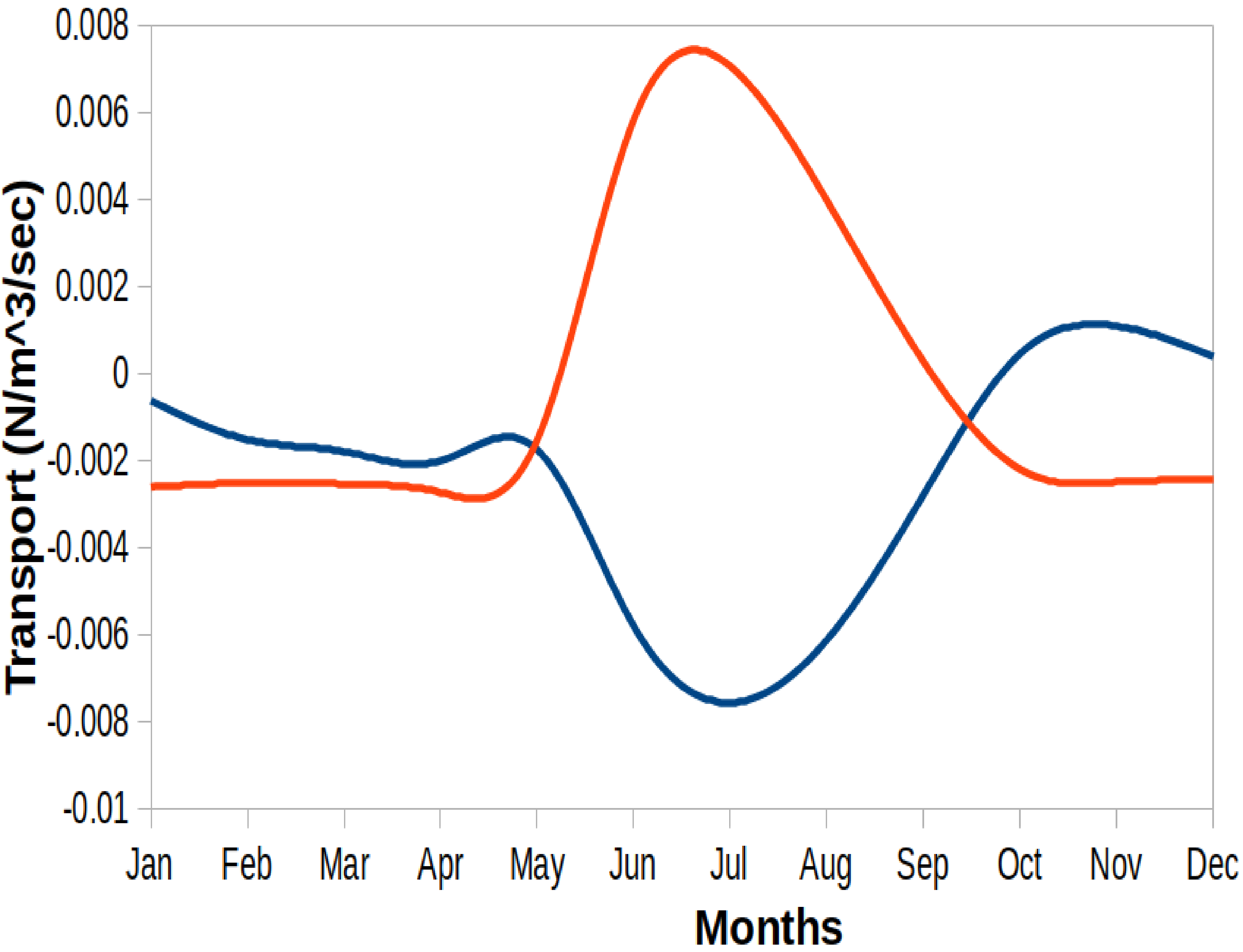

Fig.4- Using SODA dataset, Time Series of Mixed layer depth (MLD) for the 1980-2015 period area averaged over the region having coordinates 54 ^{0}E – 63 ^{0}E, 14 ^{0}N- 18 ^{0}N.

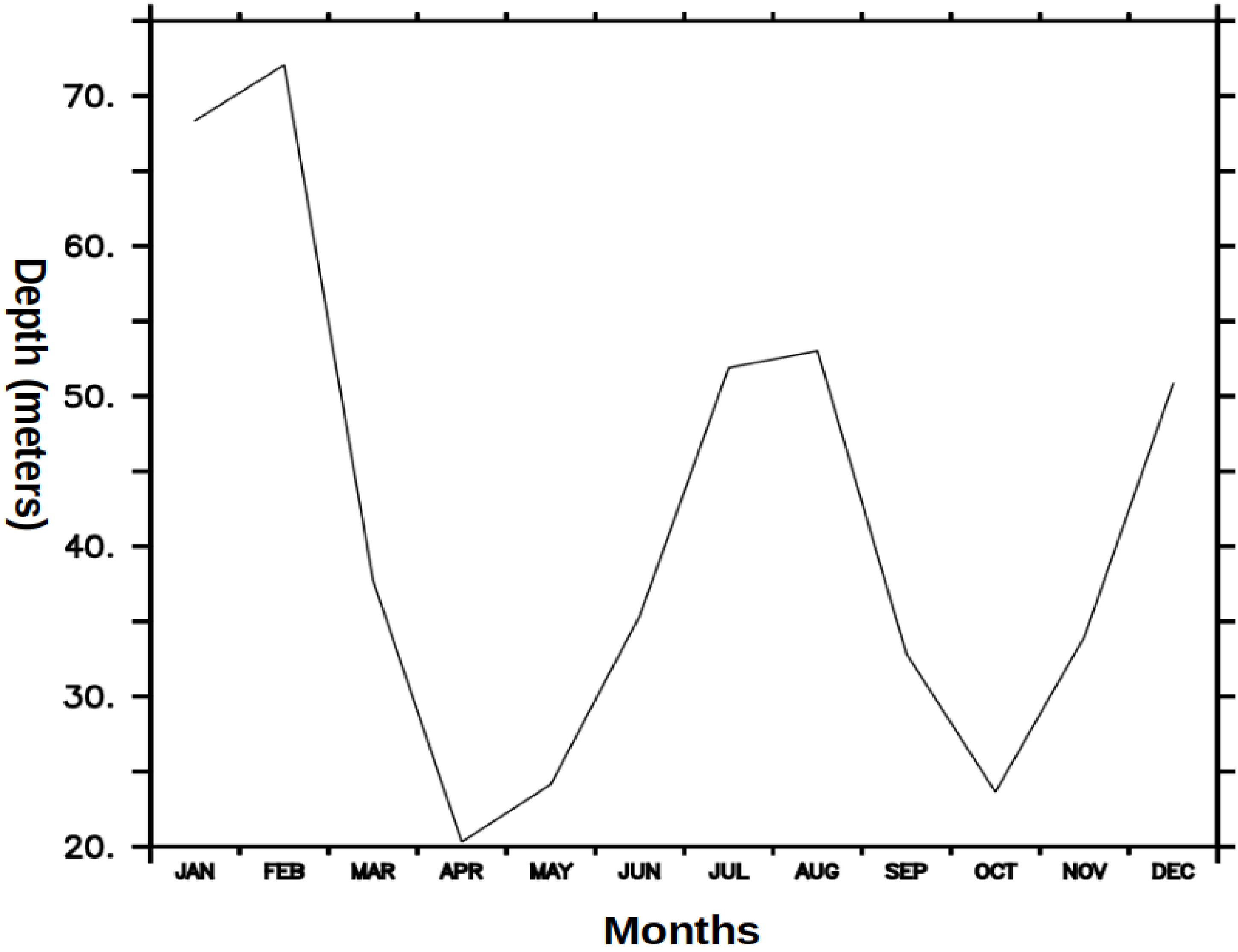

Fig.5- Climatology of Wind Stress Curl for the 1980-2015 period during January- December using SODA dataset.

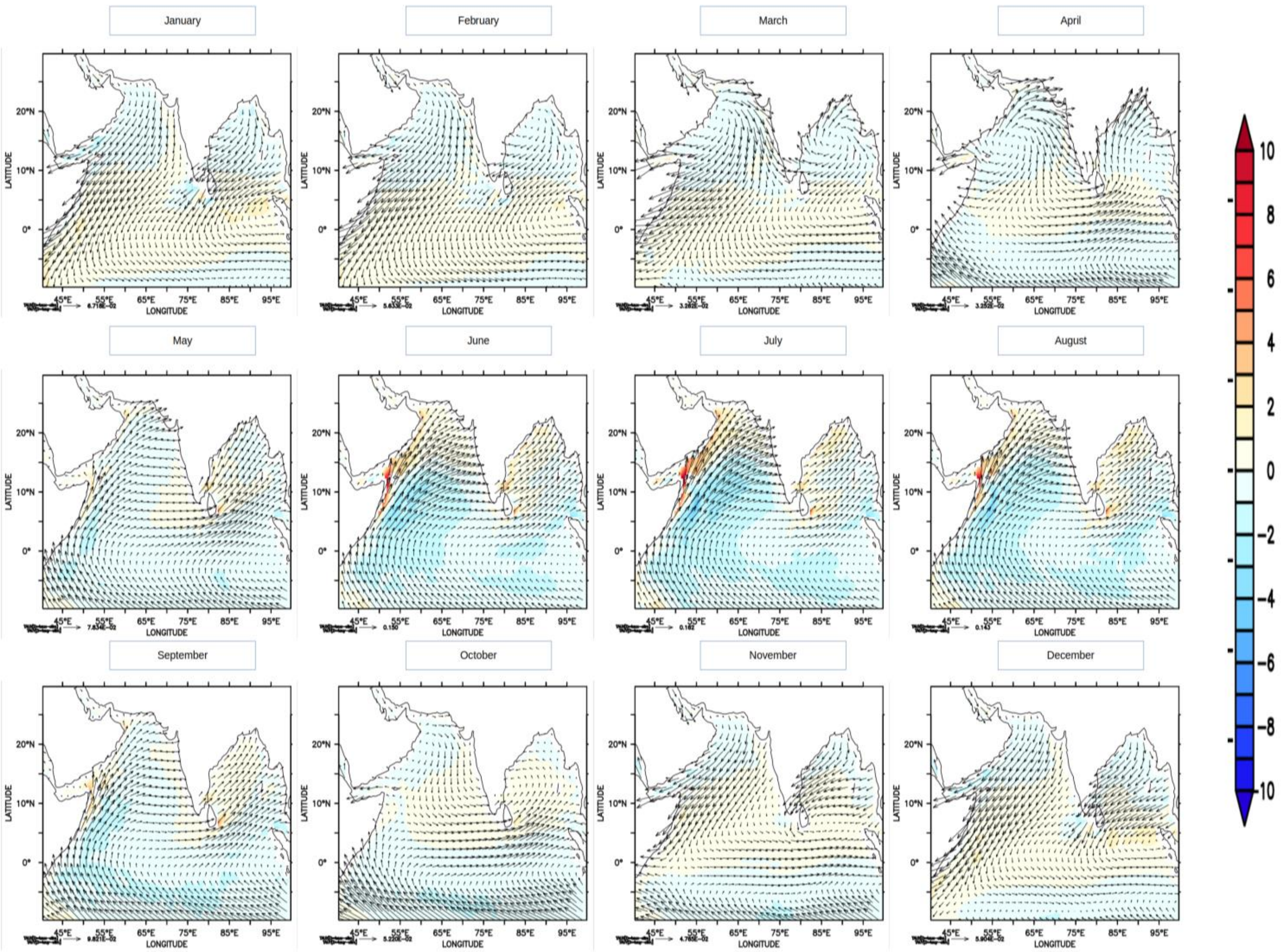

Fig.6- Correlation of wind stress with ISMR during JJAS peiod.

(a) Correlation of U component of wind stress with ISMR. (b) Correlation of V component of wind stress with ISMR.